PAPER 32 – Development of Fault Ride-Through Capability of Doubly Fed Induction Generator-Based Wind Turbine System under Fault Condition

Muhammad Abdulhadi, N. Abdulazeez, A. S. Abubakar, G. S. Shehu

Department of Electrical Engineering, Faculty of Engineering, Ahmadu Bello University, Zaria-Nigeria.

Email: abdulazeeznurudeen224@gmail.com

ABSTRACT The rapid growth in the wind power market among other Renewable energy sources (RES) is attracting the attention of scientists and researchers because the integration of Wind Turbine Systems (WTs) with the grid to complement the conventional sources in meeting up with global electrical energy demand is becoming a challenging task. The Doubly Fed Induction Generator (DFIG) has become very popular due to its low converter rating and flexible control of its active and reactive power, higher power quality, and better dynamic performance. Consequently, protecting the DFIG-based WTs from grid faults turn out to be indispensable. In this study, a 2 MW grid-connected DFIG-based WT model with a Hybrid scheme for Fault Ride-Through (FRT) capability and stability improvement was developed. The design and simulation were performed in MATLAB/Simulink (R2019b) software. The test system was subjected to disturbances leading to High Voltage Ride – Through (HVRT) by applying three–phase balanced fault without any compensation device than with conventional R-type SSFCL and finally with the Hybrid scheme. The performance of the Hybrid scheme shows fault current limitation and voltage compensation improvement over the R-type SSFCL. The THD of supply voltages with the Hybrid scheme is lower than 5%. This indicates that the Hybrid scheme complied with IEEE519 for harmonics content in power supplies.

KEYWORDS: DFIG, DC Chopper, Energy Storage, Fault current limiter (FCL), Fault Ride-Through, R-type SFCL,

1. INTRODUCTION

Wind energy amid several sustainable renewable energy sources (RES) that include hydro, solar (photovoltaic), tidal, biomass and geothermal, has become the most widespread energy source as a result of its cheap cost of maintenance, high production ability, availability in numerous parts of the world and absence of air pollution. Also, wind power is an intermittent energy source in the power system network but with this effect over 666GW of power would be generated worldwide using wind energy source in 2019 (Hossain, 2018). Electrical energy generation using Wind Turbine (WT) is accomplished by means of different configurations of induction or synchronous generators in connection with power electronic devices (Gardner *et al*., 2012). The most commonly used generator for wind turbine system are: Squirrel Cage Induction Generation (SCIG); Permanent Magnet Synchronous Generator (PMSG); Brushless Doubly Fed Induction Generator (BDIG; and Doubly Fed Induction Generator (DFIG). The DFIG becomes the most preferable for WT system owing to its merits which include reduced mechanical stress, pliable control of active and reactive power, variable speed operation, and low power rating of the connected power electronics converters (Amalorpavaraj *et al*., 2017). Conversely, one of the main drawback of the grid-connected DFIG-based WT is that it is very difficult to improve the performance of the DFIG via weakening the flux due to the fact that the stator of the DFIG is connected directly to the grid where the grid voltage directly controls the stator flux as such, a current surge is produced in rotor side converter (RSC) due to sudden change in machine magnetization caused by any voltage dip (Zhu *et al*., 2017). As a result of the large share of WT in supplying electric power to the grid and maintaining the overall system reliability, most countries necessitated that DFIG-based WT systems remain coupled to the grid in case of fault for certain period so as to satisfy condition of grid code (Fault Ride Through) (Xiao *et al*., 2018). Grid code states that wind farms must remain coupled to the grid for a certain period of time during fault and offer reactive power support to voltage dip (Alaraifi *et al*., 2013). Strictly, wind farm should adhere to the grid code since its disconnection leads to destabilization of the grid. The sensitivity of DFIG-based WT system due to the direct connection of its stator with the grid and the impact of fault current on the rotor, lead to large rotor current to be developed. The large current inrush in the rotor side causes the failure of the rotor side converter (RSC), destabilizes the DC-link voltage and DFIG eventually loses control (Uddin *et al*., 2017). The destabilized DC-link voltage decreases the life span of DC-link capacitor and reduces the efficiency of the converters (Amalorpavaraj et al., 2017).

Control improvement and hardware modification are the two existing method of enhancing the FRT (Xiao *et al*., 2018). Some techniques have been developed to minimize the overcurrent through grid fault or Transient stability (TS) of wind turbine by modelling grid side converter (GSC) or RSC control such as dual control and demagnetizing current control techniques (Alaraifi *et al*., 2013; Xiao *et al*., 2018).

Conventional crowbar is one of the hardware solutions that has been used to divert the overcurrent to power dissipated resistive circuit from RSC (Tohidi & Behnam, 2016; Uddin *et al*., 2017). Even though the current is diverted from converter using this method, but the generator acts as an induction machine that takes reactive power from the grid (Uddin *et al*., 2017). The DC chopper strategy is also commonly used to decrease the rotor overcurrent and to decrease the DC-link overvoltage for improving the operational safety of WT (Xiao *et al*., 2018). Conversely, this techniques is unable to arrest the oscillation of electromagnetic torque which might be destructive to the gearbox in some exciting situations (Nataraj *et al*., 2018; Yasoda *et al*., 2016).

DC chopper associated with storage system is implemented to prevent overvoltage in DC-link capacitor (Abbey & Joos, 2007; Uddin *et al*., 2017). A resistive type solid state fault current limiter (R-type SSFCL) is also used to enhance the capability of DFIG in FRT by withstanding fault up to a small duration but its limitation transpires during long duration faults (Dai *et al*., 2016; Uddin *et al*., 2017). Temporarily, R-type SSFCL scheme can only decrease the peak value of rotor fault current, but it doesn't have capability to remove the back EMF in rotor windings which is induced from transient stator flux and lead to a stator frequency plus rotor harmonics in rotor windings (Zou et al., 2016).

In order to decrease the negative impact of varying wind speed to DFIG output active power, shorten the recovery time after grid fault, limit the short-circuit current during faults and improve the transient stability of the system simultaneously, this paper implements a hybrid scheme which composes of R-type SSFCL, Energy Storage System (ESS) and DC chopper (DC-C) with modified control of RSC. The advantages of different schemes are combined to achieve a better response. The hybrid scheme aimed to have the ability of protecting RSC and DC-link capacitor by limiting the fault current and damp out the transients quickly. The scheme is also intended to smooth electromagnetic torque by reducing the mechanical stress on the WT.

2. THEORETICAL ANALYSIS

2.1 Concept of Doubly Fed Induction Generator DFIG

The DFIG is basically a wound rotor induction machine in which both stator and rotor are connected to electrical sources – thus the term 'doubly fed'. The dynamic model, operation and control of DFIG are discussed below.

Model of DFIG

The dynamic model of DFIG is fundamentally based on the general machine model in synchronous reference frame and all the system parameters and variables in per unit (p.u) and referred to the stator side (Rahimi & Parniani, 2010). Figure 1 shows the equivalent circuit of the DFIG in synchronous dq reference frame.

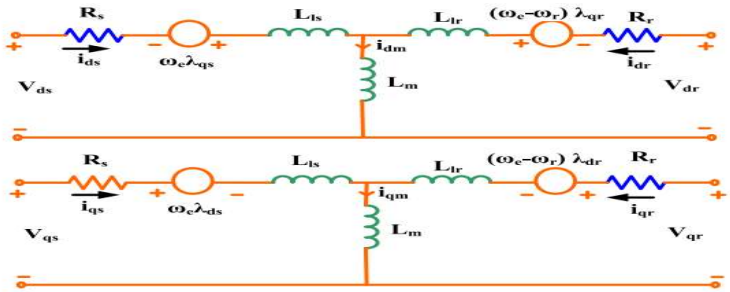

Figure 1: Equivalent Circuit of DFIG (Alaraifi *et al.,* 2013)

The dq voltage, current and flux equations of the equivalent circuit of DFIG are as follows (Amalorpavaraj *et al.,* 2017):

$$v_{ds} = R_s i_{ds} + \frac{d\lambda_{ds}}{dt} - \omega_e \lambda_{qs} \quad (1)$$

$$v_{qs} = R_s i_{qs} + \frac{d\lambda_{qs}}{dt} + \omega_e \lambda_{ds} \quad (2)$$

$$v_{dr} = R_r i_{dr} + \frac{d\lambda_{dr}}{dt} - (\omega_e - \omega_r)\lambda_{qr} \quad (3)$$

$$v_{qr} = R_r i_{qr} + \frac{d\lambda_{qr}}{dt} + (\omega_e - \omega_r)\lambda_{dr} \quad (4)$$

Where: $\mathbf{v_{ds}}$ and $\mathbf{v_{qs}}$ are dq stator voltages, $\mathbf{v_{dr}}$ and $\mathbf{v_{qr}}$ are dq rotor voltages; $\mathbf{i_{ds}}$ and $\mathbf{i_{qs}}$ are dq stator currents, $\mathbf{i_{dr}}$ and $\mathbf{i_{qr}}$ are dq rotor currents; ω_e is the supply angular frequency and ω_r is the rotor angular frequency; $\lambda_{\mathbf{ds}}$ *and* $\lambda_{\mathbf{qs}}$ are the dq stator flux linkages, $\lambda_{\mathbf{dr}}$ and $\lambda_{\mathbf{qr}}$ are the dq rotor flux linkages. $\mathbf{R_s}$ and $\mathbf{R_r}$ are the stator and rotor resistance respectively.

If L_s and L_r represent the stator and rotor inductance respectively, then the stator and rotor side inductances can be obtained using:

$$L_s = L_{ls} + L_m \quad (5)$$

$$L_r = L_{lr} + L_m \quad (6)$$

Where: L_{ls} and L_{lr} are the stator and rotor leakage inductance respectively and L_m is the magnetizing inductance.

The flux linkage equations for both stator and rotor are given by

$$\lambda_{ds} = L_s i_{ds} + L_m i_{dr} \quad (7)$$

$$\lambda_{qs} = L_s i_{qs} + L_m i_{qr} \quad (8)$$

$$\lambda_{dr} = L_m i_{ds} + L_r i_{dr} \quad (9)$$

$$\lambda_{qr} = L_m i_{qs} + L_r i_{qr} \quad (10)$$

The real power (P_s) and reactive power (Q_s) generated by DFIG are given by

$$P_s = \frac{3}{2}\left(v_{qs} i_{qs} + v_{ds} i_{ds}\right) \quad (11)$$

$$Q_s = \frac{3}{2}\left(v_{qs} i_{ds} - v_{ds} i_{qs}\right) \quad (12)$$

Operating Principle of DFIG

The operational analysis of DFIG in transient and steady state conditions is very significant to understanding its performance under grid faults. The fault analysis is essential for the implementation of FRT capability (Amalorpavaraj *et al.,* 2017). It has been stated that the stator of DFIG is directly connected to the grid while its rotor is connected to the grid through slip rings over a partial-scale back-to-back power converter. The back-to-back converter composed of a RSC and GSC connected to a dc-link. The dc-link is basically a capacitor which aids as energy storage and also serves as dc-link voltage ripples limiter. The converter converts within 20 – 30 % of total generated power. It also controls torque, speed and reactive power to or from the grid (Alsmadi *et al.,* 2018). The three-phase windings of the rotor are energized through three-phase current which is supplied via the RSC. Consequently, the rotor magnetic field interacts with stator magnetic field to develop torque as a vector product of the two vector fields (Fletcher *et al.,* 2010).

Control of DFIG

The control of DFIG functions essentially to regulate the power extracted from the WT, limit the power during high wind speed and to adjust the exchange of reactive power between the WT system and the grid. The control involves pitch control for the turbine, RSC and GSC control for the DFIG (Wessels *et al*., 2011). The rotor current controls the RSC which varies the torque and excitation while the GSC ensures constant dc-link voltage (Uddin *et al*., 2017). Figure 2 shows the control block diagram of DFIG. Many DFIGs deploy close-loop current control using Voltage Source Inverter (VSI) or vector-control technique.

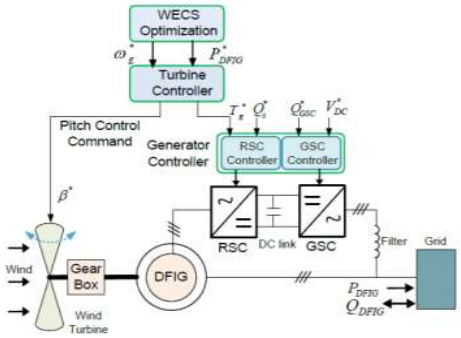

Figure 2: Control Block Diagram of DFIG-based WT (Wessels *et al*., 2011)

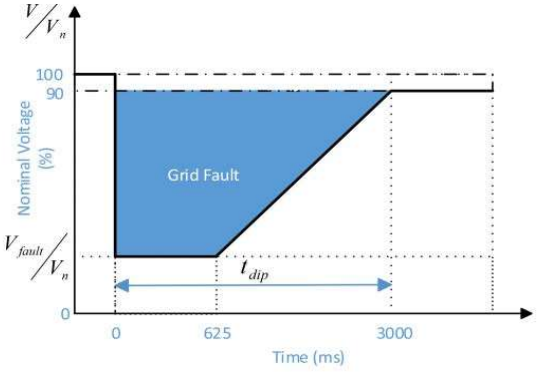

Figure 2: Figure 3: Grid Code FRT Requirement for WTs (Uddin *et al.,* 2017).

Grid Codes and FRT Requirement of DFIG

The requirements are as follows:

1. WT must stay connected to the grid for certain time (determined by the system specifications);
2. Active power must be restored immediately after the fault clearance; and
3. WT must provide reactive power thereby supporting the grid voltage during the fault (Ambati *et al.,* 2015).

Figure 3 shows the grid code FRT requirement.

3. Methodology

The methodology adopted in this research towards developing a hybrid scheme comprising of BSFCL, DC chopper and energy storage system for improving the fault ride through (FRT) and transient stability of grid connected DFIG-based WTs are discussed.

3.1 Modelling of the DFIG – Based WT

The DFIG model used in this paper was accomplished using equation (1 - 12). The DFIG Simulink model is as shown in Appendix B.

3.2 Modelling of the Grid

The DFIG – Based WT system integrated to the grid and its components were modelled as presented in Appendix C. In the model, bus 1 with nominal voltage of 600V was connected to the terminals of the DFIG. The 63kV/600V transformer was used to step up the voltage of the DFIG to a nominal grid voltage of 63kV for secondary transmission.

The grid taken as a 25km transmission line block was modelled with a single PI section. The model comprises of one set of RL series element connected between input and output terminals and two sets of shunt capacitances lumped at both ends of the line. RLC components are calculated using hyperbolic modifications to yield precise representations in zero and positive-sequence at specified frequencies. In order to achieve a stretched frequency response, a distributed parameter line was used in the model.

3.3 Energy Storage System and DC – Link Capacitor

The ideal dc voltage source and the dc – link capacitor parameters are, a 5000V was taken as the maximum voltage of the dc source with a 10Ω series resistance and 10000e-6 as the capacitance of the dc – link capacitor with an initial voltage of 1150V.

3.4 Fault Current Limiter (FCL)

The Fault Current Limiter employed has a switch model controlled by a gate signal and a virtual impedance. When in ON-state the switch model has an internal resistance (R_{on}). In OFF-state, this internal resistance is infinite. When the gate signal (g) is set to 1, the switch model is ON-state. A diode in parallel with a series RC snubber circuit having R_{on} and (L_{on}) at ON-state is also integrated. R_{on} being carefully chosen as $1 \times 10^{-3}\Omega$ and the Snubber resistance as $10^{3}\Omega$ were adopted from Beheshtaein et al., 2017 for both the controlled switch and diode respectively. The Diode impedance was infinite in OFF-state mode. The limiting fault current is expressed as (13).

$$I_{lim}^{m}(t) = \frac{U_s(t)}{Z_s + Z_{lim}} \approx \frac{U_s(t)}{Z_{lim}} \quad (13)$$

Where: Z_{lim} is the limiting impedance, $U_s(t)$ is the voltage of secondary transformer. It is assumed that $Z_s \ll Z_{lim}$.

A PI current controller and an active damping loop were realized to sense and trigger the control scheme. For mitigation, the current measurements was accomplished using Multiple Second – Order Generalized integrators PLL (MSOGI-PLL) for its fast response and less computational burden. Appendix D illustrates the employed FCL block with its components.

4. RESULTS AND DISCUSSION

The performance of the Hybrid scheme and the conventional R-type SSFCL in ensuring FRT ability was established by injecting grid faults (single-phase to ground faults) into the system. For fault considered in the work, the situation of voltage sag was accomplished by means of switching a highly inductive load at 0.3 seconds while the deeper voltage sag was achieved by means of a fault implementation block in MATLAB/Simulink environment. The fault was chosen between any phase and the ground. The switching time was also chosen between 0.4 to 0.6seconds while the fault resistance and ground resistance were both selected to be 0.0001Ω. Additionally, a snubber resistance of 1MΩ and infinite snubber capacitance were selected for a more severe fault condition. Lastly, a capacitive load was switched ON at 0.6 seconds to give the voltage swell. The supply voltage RMS values at PCC, the DFIG stator current response, DFIG electromagnetic torque, rotor speed of DFIG, DFIG rotor current response, and DC – Link voltage through Unbalanced Fault (Single-Phase to Ground) are shown in Figure 5-11 respectively.

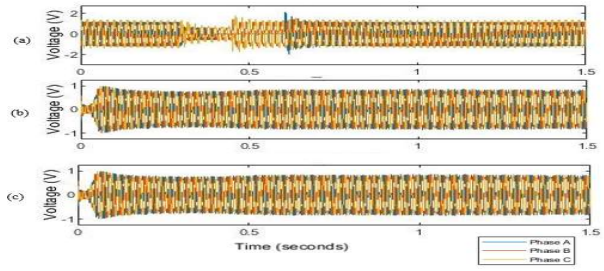

Figure 5: Unbalanced Fault (single phase to ground) supply Voltage

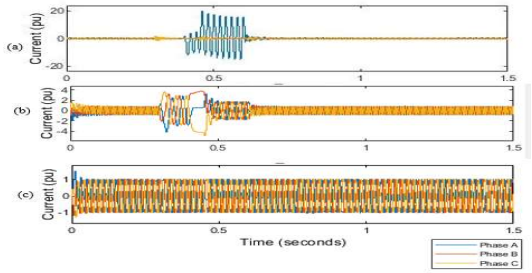

Figure 6: DFIG stator current response after applying a temporary unbalanced single-phase to ground fault

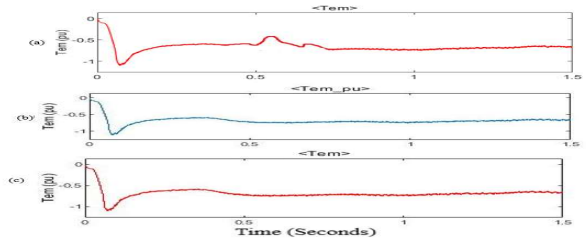

Figure 7: Electromagnetic Torque (Tem) response curves of the DFIG (single phase to ground) supply Voltage

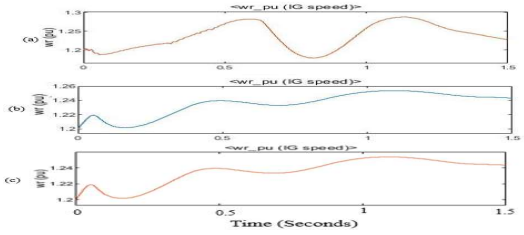

Figure 8: DFIG Rotor Speed under Unbalanced Fault (single phase to ground) supply Voltage

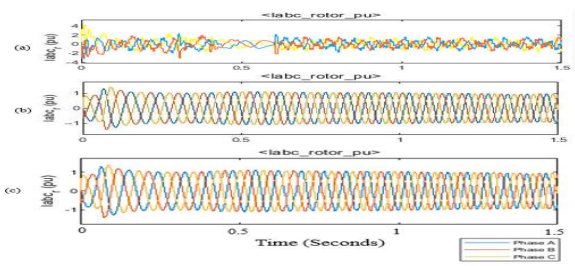

Figure 9: DFIG Rotor Current under Unbalanced Fault (single phase to ground) supply Voltage

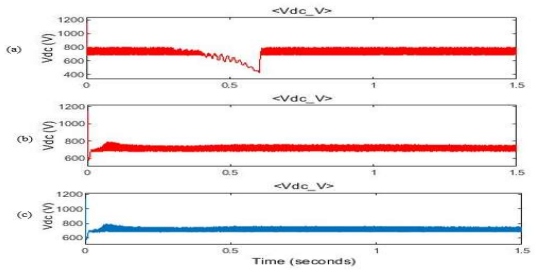

Figure 10: DC-link Voltage during Unbalanced Fault (single phase to ground) supply Voltage

It can be observed that the proposed hybrid scheme performed well and has the capability to improve the transient stability of the DFIG based variable speed WG system for unbalanced single-phase to ground faults as shown in Table 1-4. The voltage level is maintained at ±0.1 p.u. of the nominal value at PCC point and can mitigate the high current significantly during the fault time compared to R-type SSFCL scheme. The hybrid scheme also, stabilizes the machine speed during a fault, thus DFIG faces low stress and improves the transient stability. The THD (%) of supply voltage are 29.93pu, 4.01pu and 1.01pu without any compensation device, with R-type SSFCL and Hybrid scheme respectively. The percentage improvement in the voltage when Hybrid scheme was used was, 75.37% compared to that of R-type SSFCL. Correspondingly, the percentage decrease in output current profile was approximated to about 87.20%.

Table 1: Performance indices values for unbalanced single-phase to ground fault

Index Parameters	**Indices values for Unbalanced 1LG**		
	No Control	With R-type SSFCL	With Hybrid Scheme
Voltage (pu)	2.10	0.92	0.92
Speed (pu)	1.18	1.20	1.21
V_{dc} (V)	415	715	720

Table 2: Transient Stability Improvement for unbalanced single-phase to ground fault

Transient Criteria	**Improvement Comparison for Unbalance 1LG fault**	
	With R-type SSFCL	With Hybrid Scheme
Voltage	High	High
Speed	Moderate	High
Power	Moderate	High
DC link voltage	High	High

Table 3: Comparison among the series devices for the percentage of THD

Parameters	**Controller**	**Performance**	
		THD (%)	Improvement
Voltage	Hybrid Scheme	1.01	75.37%
	R-type SSFCL	4.10	

Table 4: Comparison among the series devices for the percentage TRD

Parameters	**Controller**	**Performance**	
		TRD (%)	Improvement
Current	Hybrid Scheme	1.01	87. 20%
	R-type SSFCL	7.89	

5. CONCLUSION

This paper developed a hybrid scheme consisting of Resistive-type Solid-state Fault Current Limiter (R-type SSFCL), Breaking Chopper (BC) and Energy Storage System (ESS) for Doubly-Fed Induction Generator (DFIG) based Wind Turbine (WT) system. The developed scheme focused on enhancing Fault Ride-Through (FRT) capability of DFIG based WT through the Hybrid scheme thus protecting the strict grid code requirements for the WT integration to grid networks. The scheme also guaranteed the protection of the converters against short-circuit currents. The Hybrid scheme performance indicates that there was an improvement in terms of fault current mitigation and voltage compensation over R-type SSFCL thus making the Hybrid scheme a better option for guaranteeing an improved DFIG-based WT systems FRT capability.

REFERENCES

Abbey, C., & Joos, G. (2007). Supercapacitor Energy Storage for Wind Energy Applications. *IEEE Transactions on Industry Applications*, *43*(3), 769–776. https://doi.org/10.1109/TIA.2007.895768

Alaraifi, S., Moawwad, A., El Moursi, M. S., & Khadkikar, V. (2013). Voltage Booster Schemes for Fault Ride-Through Enhancement of Variable Speed Wind Turbines. *IEEE Transactions on Sustainable Energy*, *4*(4), 1071–1081. https://doi.org/10.1109/TSTE.2013.2267017

Alsmadi, Y. M., Xu, L., Blaabjerg, F., Ortega, A. J. P., Abdelaziz, A. Y., Wang, A., & Albataineh, Z. (2018). Detailed Investigation and Performance Improvement of the Dynamic Behavior of Grid-Connected DFIG-Based Wind Turbines Under LVRT Conditions. *IEEE Transactions on Industry Applications*, *54*(5), 4795–4812. https://doi.org/10.1109/TIA.2018.2835401

Amalorpavaraj, R. A. J., Kaliannan, P., Padmanaban, S., Subramaniam, U., & Ramachandaramurthy, V. K. (2017). Improved Fault Ride Through Capability in DFIG Based Wind Turbines Using Dynamic Voltage Restorer With Combined Feed-Forward and Feed-Back Control. *IEEE Access*, *5*, 20494–20503. https://doi.org/10.1109/ACCESS.2017.2750738

Ambati, B. B., Kanjiya, P., & Khadkikar, V. (2015). A Low Component Count Series Voltage Compensation Scheme for DFIG WTs to Enhance Fault Ride-Through Capability. *IEEE Transactions on Energy Conversion*, *30*(1), 208–217. https://doi.org/10.1109/TEC.2014.2351799

Dai, S., Xiao, L., & Guo, W. (2016). Fault current limiter-battery energy storage system for the doubly-fed induction generator: analysis and experimental verification. *IET Generation, Transmission & Distribution*, *10*(3), 653–660. https://doi.org/10.1049/iet-gtd.2014.1158

Fletcher, D. J., Fletcher, D. J., & Yang, J. (2010). *Introduction to the Doubly-Fed Induction Generator for Wind Power Applications, Paths to Sustainable Energy*. 259. Retrieved from http://citeseerx.ist.psu.edu/viewdoc/summary?doi=10.1.1.725.7456

Gardner, P., Andrew, G., Lars, F. H., Colin, M., & Arthouros, Z. (2012). *Wind energy-the facts: a guide to the technology, economics and future of wind power*. New York: Earthscan.

Hossain, M. E. (2018). Improvement of transient stability of DFIG based wind generator by using of resistive solid state fault current limiter. *Ain Shams Engineering Journal*. https://doi.org/10.1016/j.asej.2017.03.014.

Nataraj, S. K.,. (2018). Improved fault ride through capability of DFIG-wind turbines using customized dynamic voltage restorer. *Sustainable Cities and Society*, *39*, 114–125. https://doi.org/10.1016/J.SCS.2018.02.008

Rahimi, M., & Parniani, M. (2010). Efficient control scheme of wind turbines with doubly fed induction generators for low-voltage ride-through capability enhancement. *IET Renewable Power Generation*, *4*(3), 242. https://doi.org/10.1049/iet-rpg.2009.0072

Tohidi, S., & Behnam, M. (2016). A comprehensive review of low voltage ride through of doubly fed induction wind generators. *Renewable and Sustainable Energy Reviews*, *57*, 412–419. https://doi.org/10.1016/J.RSER.2015.12.155

Uddin, W., Zeb, K., Tanoli, A., & Haider, A. (2017). Hardware-based hybrid scheme to improve the fault ride through capability of doubly fed induction generator under symmetrical and asymmetrical fault. *IET Generation, Transmission & Distribution*, *12*(1), 200–206. https://doi.org/10.1049/iet-gtd.2017.0578

Wessels, C., Gebhardt, F., & Fuchs, F. W. (2011). Fault Ride-Through of a DFIG Wind Turbine Using a Dynamic Voltage Restorer During Symmetrical and Asymmetrical Grid Faults. *IEEE Transactions on Power Electronics*, *26*(3), 807–815. https://doi.org/10.1109/TPEL.2010.2099133

Xiao, X.-Y., Yang, R.-H., Chen, X.-Y., Zheng, Z.-X., & Li, C.-S. (2018). Enhancing fault ride-through capability of DFIG with modified SMES-FCL and RSC control. *IET Generation, Transmission & Distribution*, *12*(1), 258–266. https://doi.org/10.1049/iet-gtd.2016.2136

Yasoda, K. G., Nanjundappan, D., & Boominathan, V. (2016). Enhancement of transient stability of distribution system with SCIG and DFIG based wind farms using STATCOM. *IET Renewable Power Generation*, *10*(8), 1171–1180. https://doi.org/10.1049/iet-rpg.2016.0022

Zhu, D., Zou, X., Deng, L., Huang, Q., Zhou, S., & Kang, Y. (2017). Inductance-Emulating Control for DFIG-Based Wind Turbine to Ride-Through Grid Faults. *IEEE Transactions on Power Electronics*, *32*(11), 8514–8525. https://doi.org/10.1109/TPEL.2016.2645791

Zou, Z.-C., Chen, X.-Y., Li, C.-S., Xiao, X.-Y., & Zhang, Y. (2016). Conceptual Design and Evaluation of a Resistive-Type SFCL for Efficient Fault Ride Through in a DFIG. *IEEE Transactions on Applied Superconductivity*, *26*(1), 1–9. https://doi.org/10.1109/TASC.2015.2507129

APPENDICES

Appendix A: Parameter of 2.0MW WT System

Items	Specifications
Generator Data	-
Synchronous speed (rev/min)	1500
Rated power (MW)	2.0
Rated line-to-line stator voltage (V_{rms})	575
Frequency (Hz)	50
Pole pair	4
Slip (s)	-0.2
R_s (pu)	0.023
L_{ls}(pu)	0.18
L_m(pu)	2.9
R'_r(pu)	0.016
L'_{lr}(pu)	0.16
Rotor nominal voltage (V_{rms}) (V)	1975
Inertia Constant H (s)	0.685
Friction factor (pu)	0.01
Converter Data	-
GSC Max. Current (pu)	0.8
GSC Coupling Inductor [L,R] (pu)	[0.3 0.003]
DC link voltage (V)	1150
DC link Capacitor (F)	10000e-6
Line filter Capacitor (for Q = 50Var) (F)	120e3
Turbine Data	-
Nominal Mechanical Output Power (MW)	2.0
Nominal wind speed at Cp Max (m/s)	11
Initial wind speed (m/s)	11
Cut in speed (m/s)	6
Cot out speed (m/s)	30

Appendix B: DFIG and Converters control parameters

Items	Specifications
Dc link regulator gains [kp, ki]	[8 400]
GSC regulator gains [kp, ki]	[0.83 5]
Speed regulator gains [kp, ki]	[3 0.6]
RSC regulator gains [kp, ki]	[0.6 8]
Q&V regulator gains [kp_Var, ki_V]	[0.05 20]
Pitch controller gain [kp]	[150]
Pitch compensation gains [kp, ki]	[3 30]
Frequency of GSC PWM carrier (Hz)	2700
Frequency of RSC PWM carrier (Hz)	1620

Appendix C: DFIG-Based Wind Turbine Simulink Model

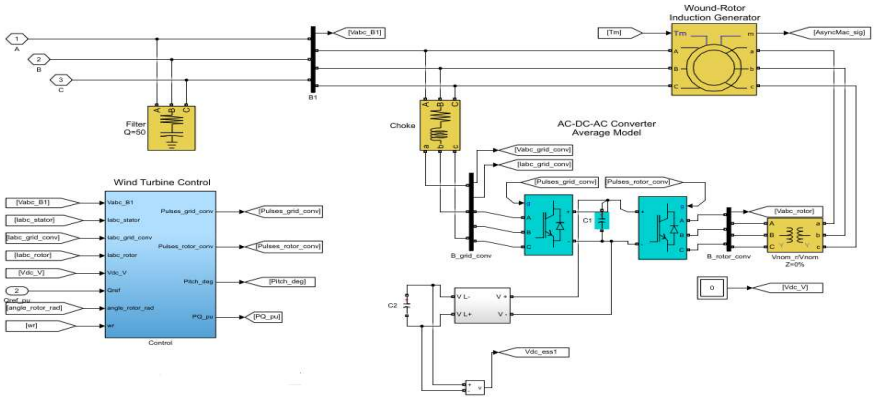

Appendix D: DFIG-Based WT System Grid Components